# Supplementary Information
# Structure of the MacAB-TolC ABC-type tripartite multidrug efflux pump

Anthony W.P. Fitzpatrick[1*], Salomé Llabrés[2], Arthur Neuberger[3], James N. Blaza[4], Xiao-chen Bai[1], Ui Okada[5], Satoshi Murakami[5], Hendrik W. van Veen[3], Ulrich Zachariae[2,6], Sjors H.W. Scheres[1+], Ben F. Luisi[7+], Dijun Du[7+*]

This supplementary file includes:

Supplementary Figure 1 to 14

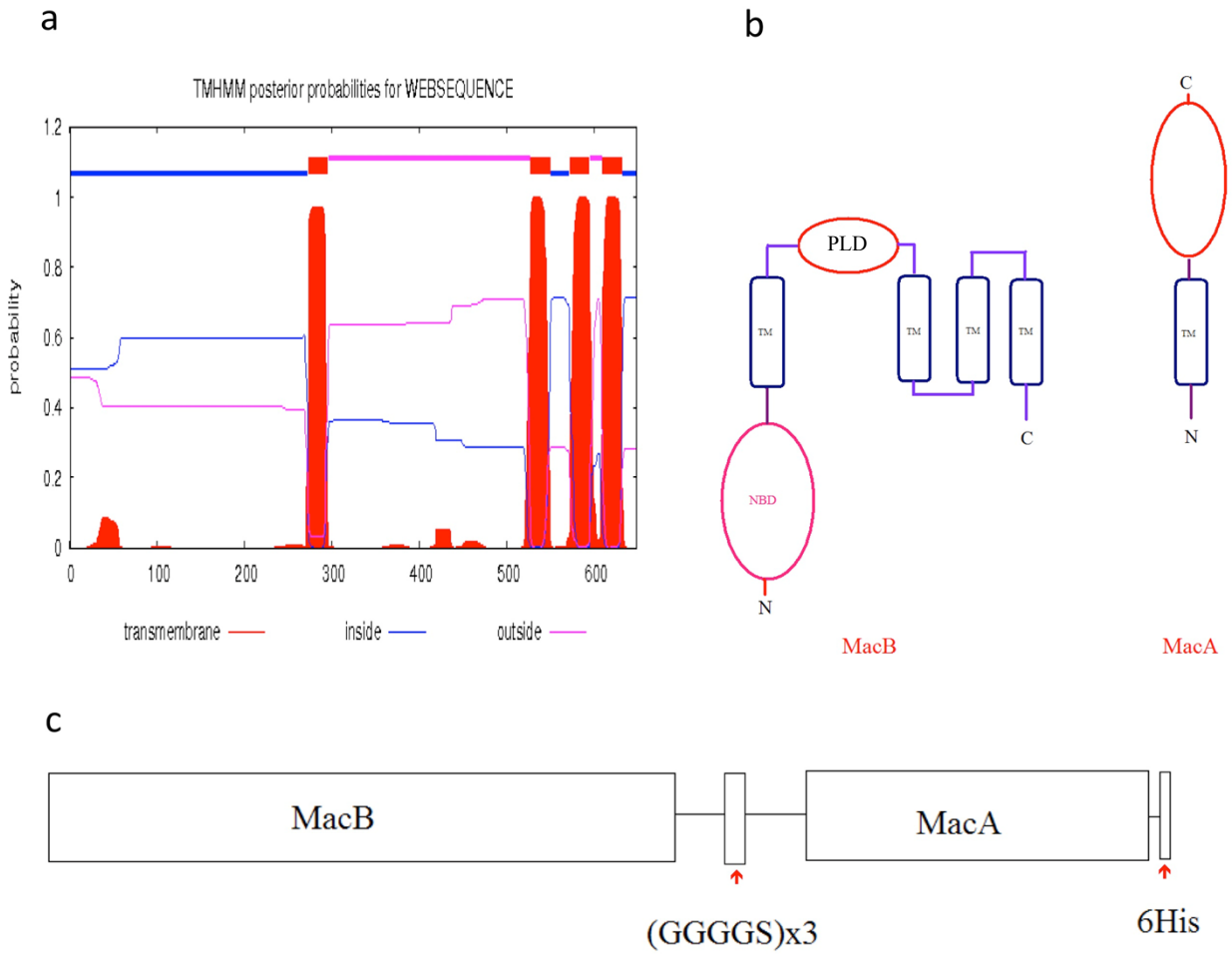


**Supplementary Figure 1 | Engineering of fusion constructs to prepare the MacA-MacB-TolC pump. a,** MacB is predicted to have 4 transmembrane spanning helices (output from TMHMM server). **b,** The nucleotide-binding domain (NBD) of MacB is located at the N-terminus of the protein. MacA has a single transmembrane helix, and the C-terminal portion has domains like those of AcrA. **c,** The fusion of MacA to the C-terminus of MacB with a flexible poly glycine-serine linker is anticipated to preserve the proper membrane topology of the components.

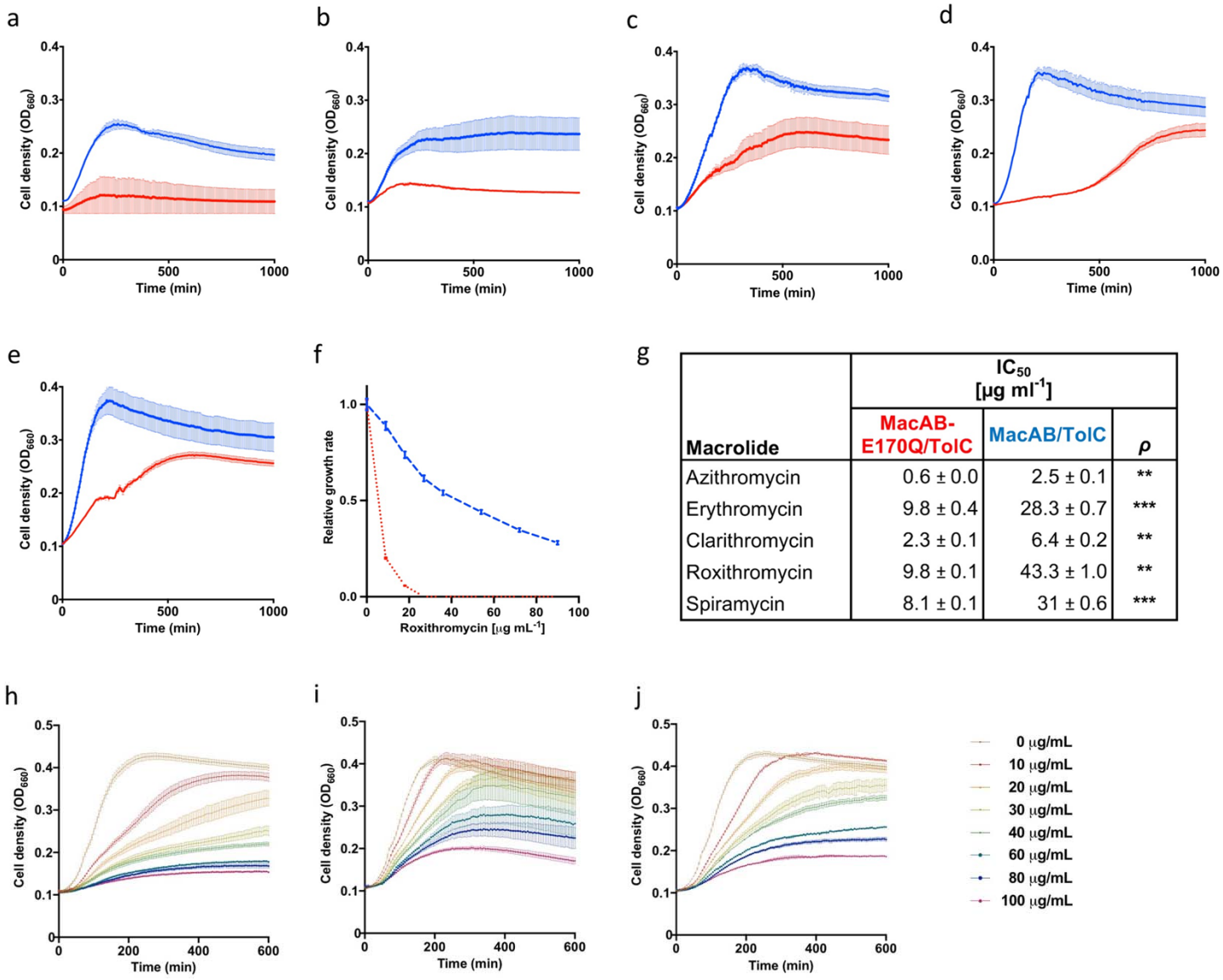


| Macrolide | $IC_{50}$ [μg ml$^{-1}$] MacAB-E170Q/TolC | MacAB/TolC | ρ |
|---|---|---|---|
| Azithromycin | 0.6 ± 0.0 | 2.5 ± 0.1 | ** |
| Erythromycin | 9.8 ± 0.4 | 28.3 ± 0.7 | *** |
| Clarithromycin | 2.3 ± 0.1 | 6.4 ± 0.2 | ** |
| Roxithromycin | 9.8 ± 0.1 | 43.3 ± 1.0 | ** |
| Spiramycin | 8.1 ± 0.1 | 31 ± 0.6 | *** |

**Supplementary Figure 2 | The engineered pumps are functionally active for drug efflux.** Growth of drug-hypersensitive *E. coli* Δ*acrAB* expressing the fused MacAB (blue) or the transport-inactive MacAB-E170Q (corresponding to MacA fused to MacB with the ATPase-inactivating Walker B E170Q mutation) (red) or in the presence of **a,** 1.2 μg ml$^{-1}$ azithromycin, **b,** 32 μg ml$^{-1}$ erythromycin, **c,** 4.6 μg ml$^{-1}$ clarithromycin, **d,** 18 μg ml$^{-1}$ roxithromycin or **e** 18 μg ml$^{-1}$ spiramycin. **f,** The growth rate of cells in the presence of a range of concentrations of the macrolide roxithromycin (0 to 90 μg ml$^{-1}$) was determined relative to the maximum growth rate in the absence of drug. From this relationship the $IC_{50}$ is defined as the drug concentration at which the relative growth rate is half-maximal. **g,** $IC_{50}$ values (± SEM) as summarized for different macrolides. (t-test stats.: **, $p < 0.01$; ***, $p < 0.001$). Drug resistance mediated by the double cysteine mutant MacA_D271C MacB_G465C. Growth of drug-hypersensitive *E. coli* Δ*acrAB* expressing **h,** MacA_D271C MacB_G465C_E170Q (transport-inactive control), **i,** wild-type MacA MacB, or **j,** MacA_D271C MacB_G465C in the presence of roxithromycin at concentrations ranging from 0 – 100 μg ml$^{-1}$. OD measurements are presented as mean of triplicate measurements ± standard error of the mean (SEM). The error bars/shaded regions represent standard error of the mean.

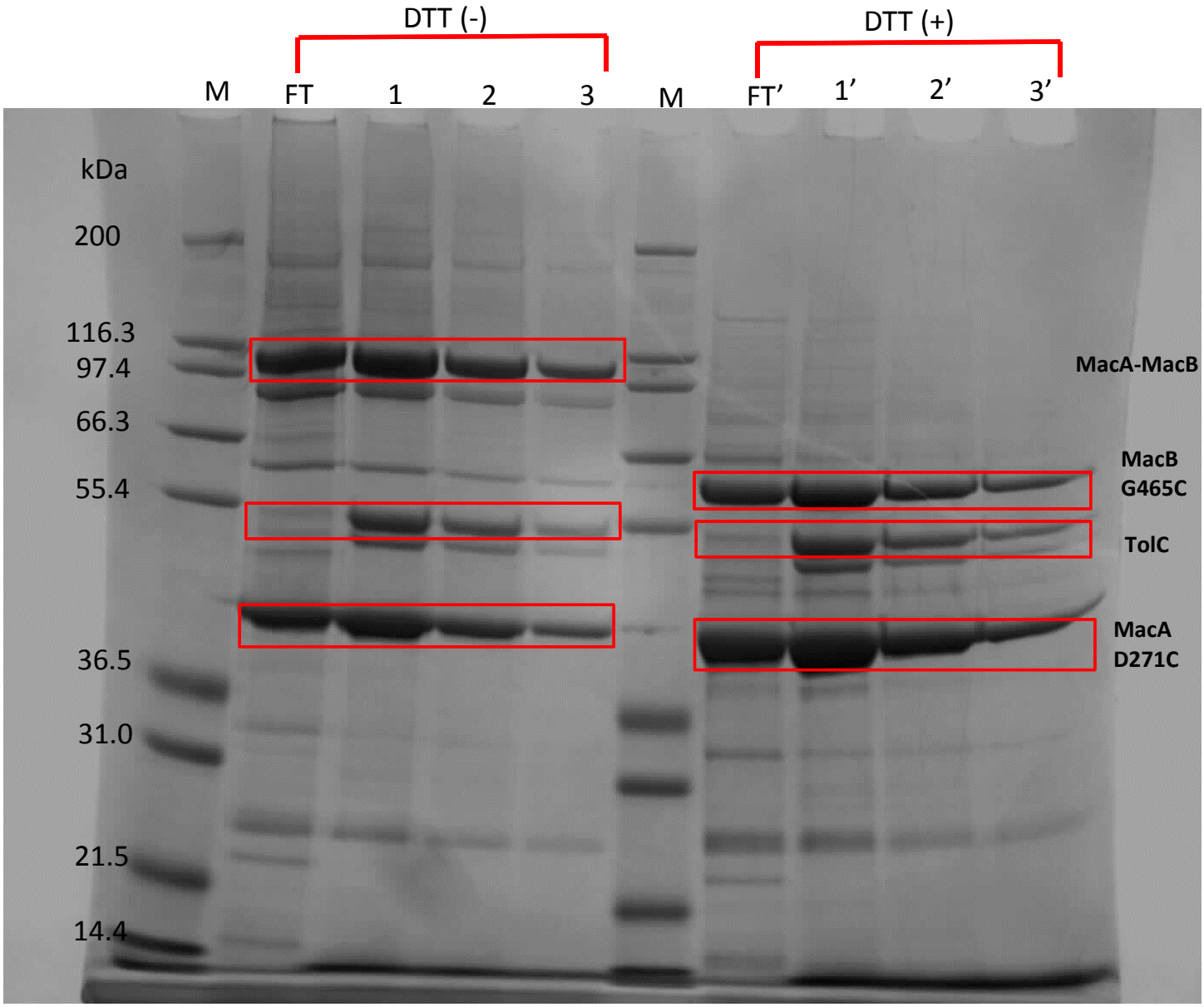


**Supplementary Figure 3 | Co-purification of MacA_D271C, MacB_G465C and TolC.** The full pump assembly was pulled down by hexa-His-tagged MacB_G465C, and was further purified by FLAG-tagged TolC. The flow-through (FT) and fractions 1-3 of the eluates by FLAG peptide were mixed with NuPAGE LDS Sample Buffer (4x) with or without 10 mM DTT and loaded on a SDS-PAGE gel.

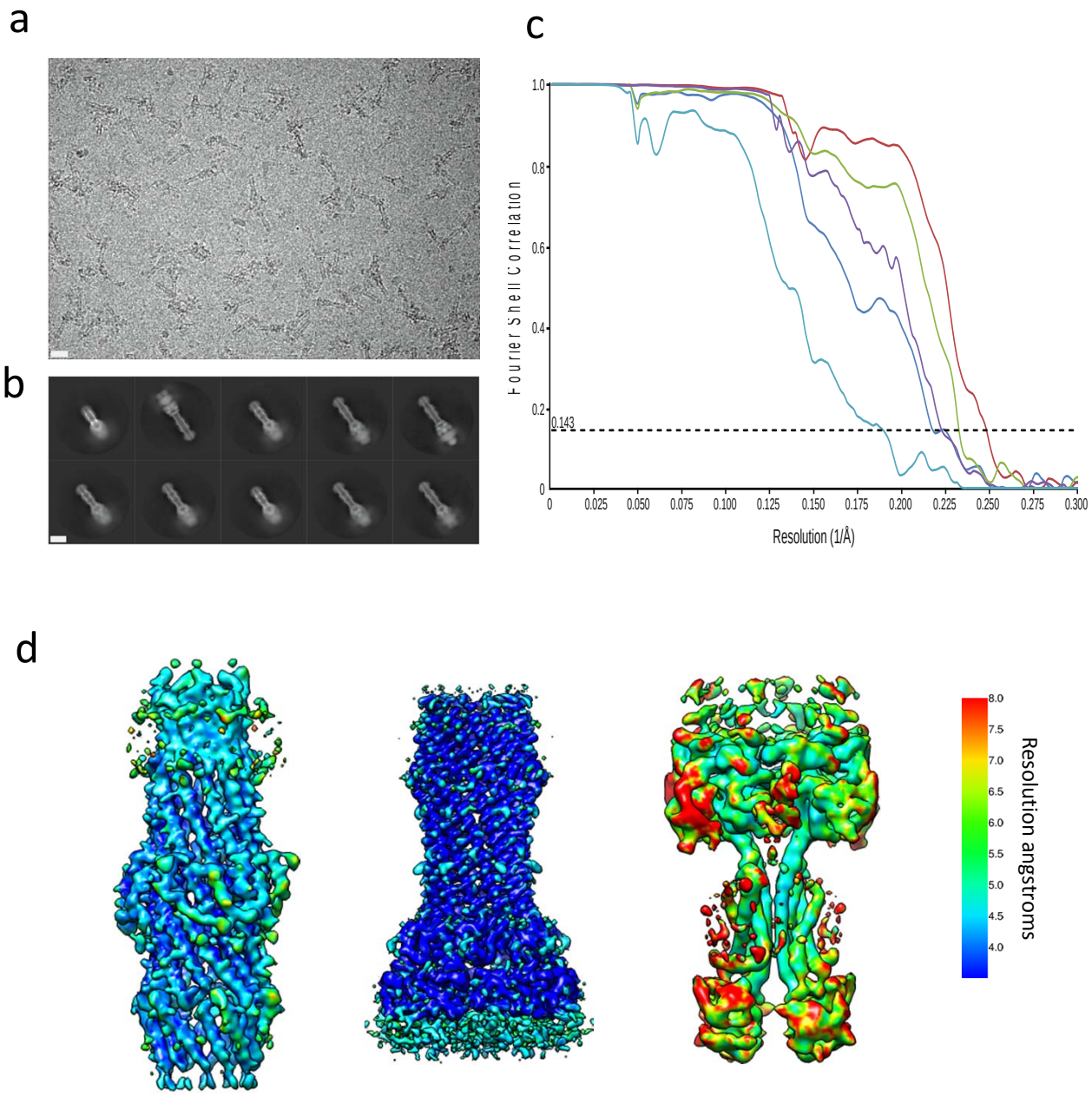


**Supplementary Figure 4 | CryoEM of the fusion-stabilised MacAB-TolC pump. a,** Representative cryoEM image of the MacAB-TolC complex. The image has been corrected for drift. (Scale bar, 200 Å). **b,** Typical two-dimensional class averages of the particles. (Scale bar, 100 Å). **c,** Gold-standard Fourier Shell Correlation indicating the resolution of the five density maps. Shown are FSC plots generated between reconstructions from random halves of the data for MacB refined with C2 symmetry (*light blue line*), TolC refined with C3 symmetry (*dark blue line*), MacA-TolC refined with C3 symmetry (*purple line*), MacA refined with C3 symmetry (*green line*) and MacA refined with C6 symmetry (*red line*). All resolutions are estimated at FSC = 0.143 (*black dashed line*). **d,** Local resolution estimation by ResMap of TolC (*left*), MacA (*middle*) and MacB (*right*). All units are in Angstrom (Å).

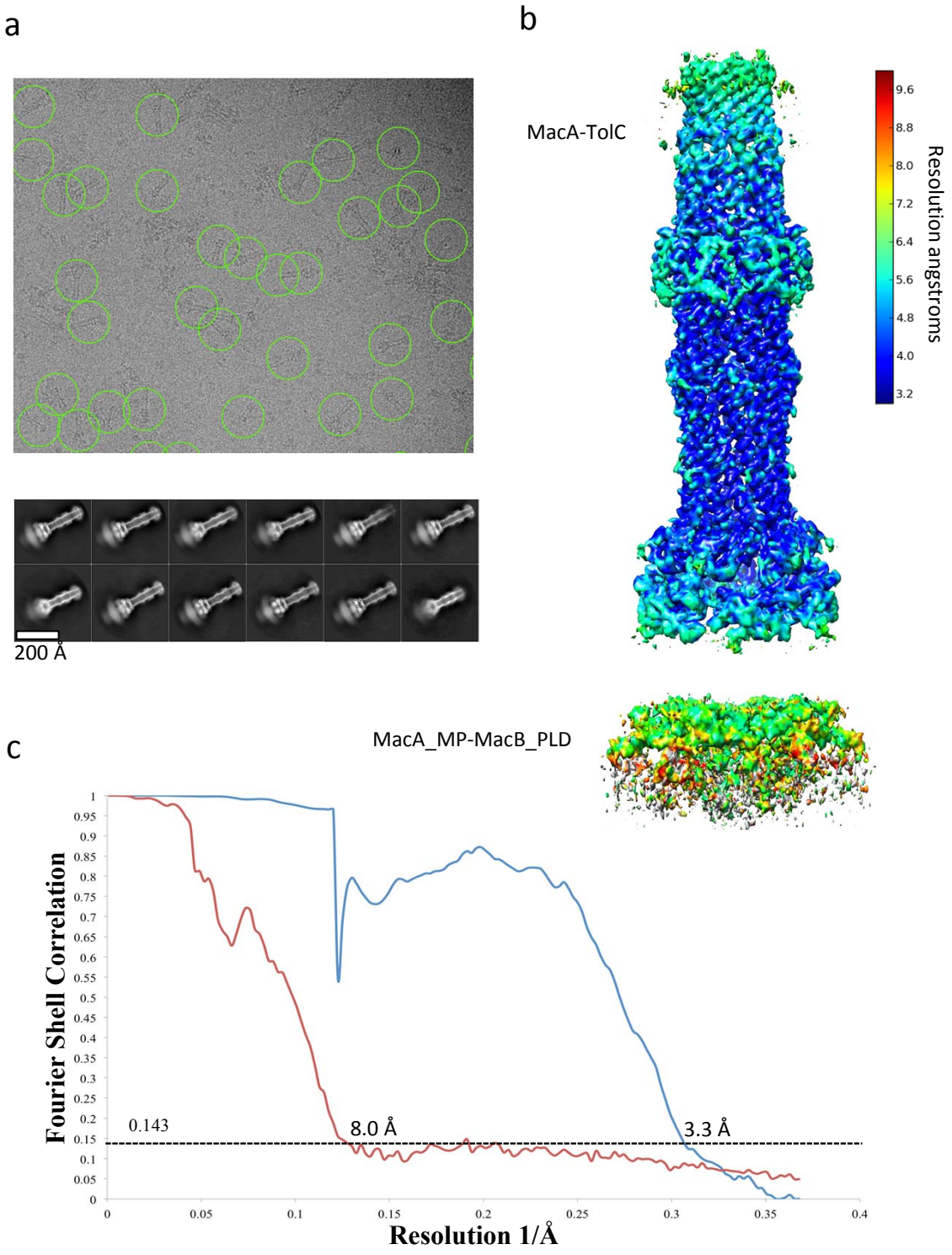


**Supplementary Figure 5 | CryoEM analysis of the disulfide-bond stabilised MacAB-TolC pump.** **a,** A representative motion-corrected cryoEM image of ice-embedded, disulfide-bond stabilised MacAB-TolC pump. Particles are circled (green). The lower panel shows reference free 2D averages calculated by Relion2.0. **b,** Colour-coded 3D maps of MacA-TolC [top] and MacA_membrane proximal domain (MP)-MacB_periplasmic domain (PLD) [bottom]based on resolution variations obtained with ResMap. **c,** Gold-standard Fourier Shell Correlation indicating the resolution of the ftwo density maps. Shown are FSC plots generated between reconstructions from random halves of the data for MacA-TolC refined with C3 symmetry (*blue line*), and MacA_MP-MacB_PLD refined with C2 symmetry (*red line*).

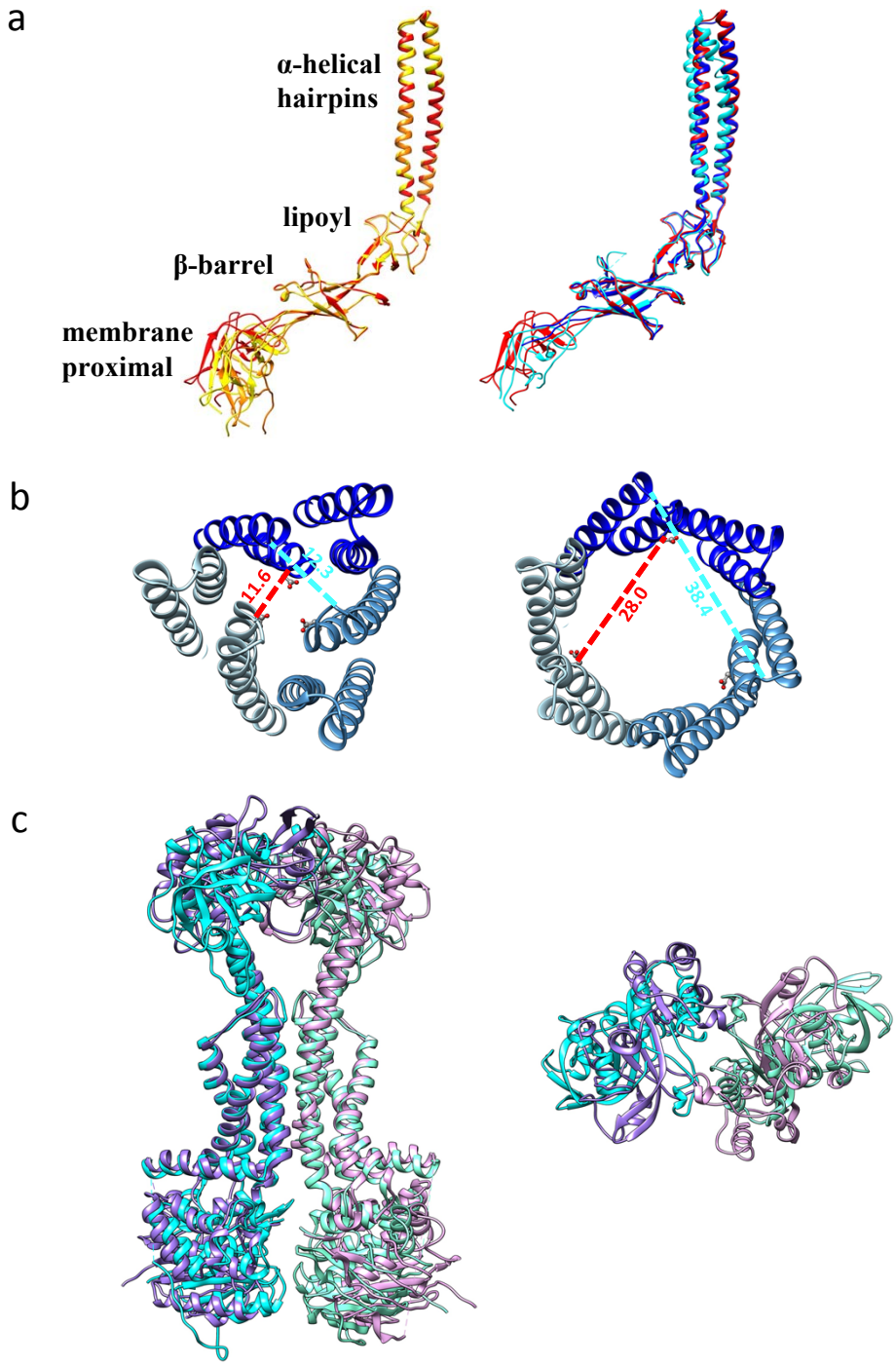


**Supplementary Figure 6 | Structure comparison of the pump components from cryo-EM and crystallography. a,** Superimposition of three MacA protomers (protomer-I: red; protomer-II: orange; protomer-IIII: yellow) in the cryo-EM structure (left), as well as protomer-I (red) with crystal structures of MacA from *E.coli* (blue, PDB code: 3FPP) and *Actinobacillus actinomycetemcomitans* (cyan, PDB code: 4DK0)(right). **b,** The periplasmic end of TolC in the crystal structure (left, PDB code: 1EK9) and cryo-EM structure (right). The dashed line in cyan shows the separation of Gly365 in adjacent subunits, which lies at the outer-most edge of the tip region. The dashed red line shows the distance of Asp374 between protomers, which form the narrowest point in the crystal structure. The distances are measured in angstroms between the Cα. **c,** Side view (left) and top view of the superimposition of the cryo-EM structure (purple) with the crystal structure (cyan) of MacB. In the top view, only the periplasmic domain of MacB is shown for clarity (right).

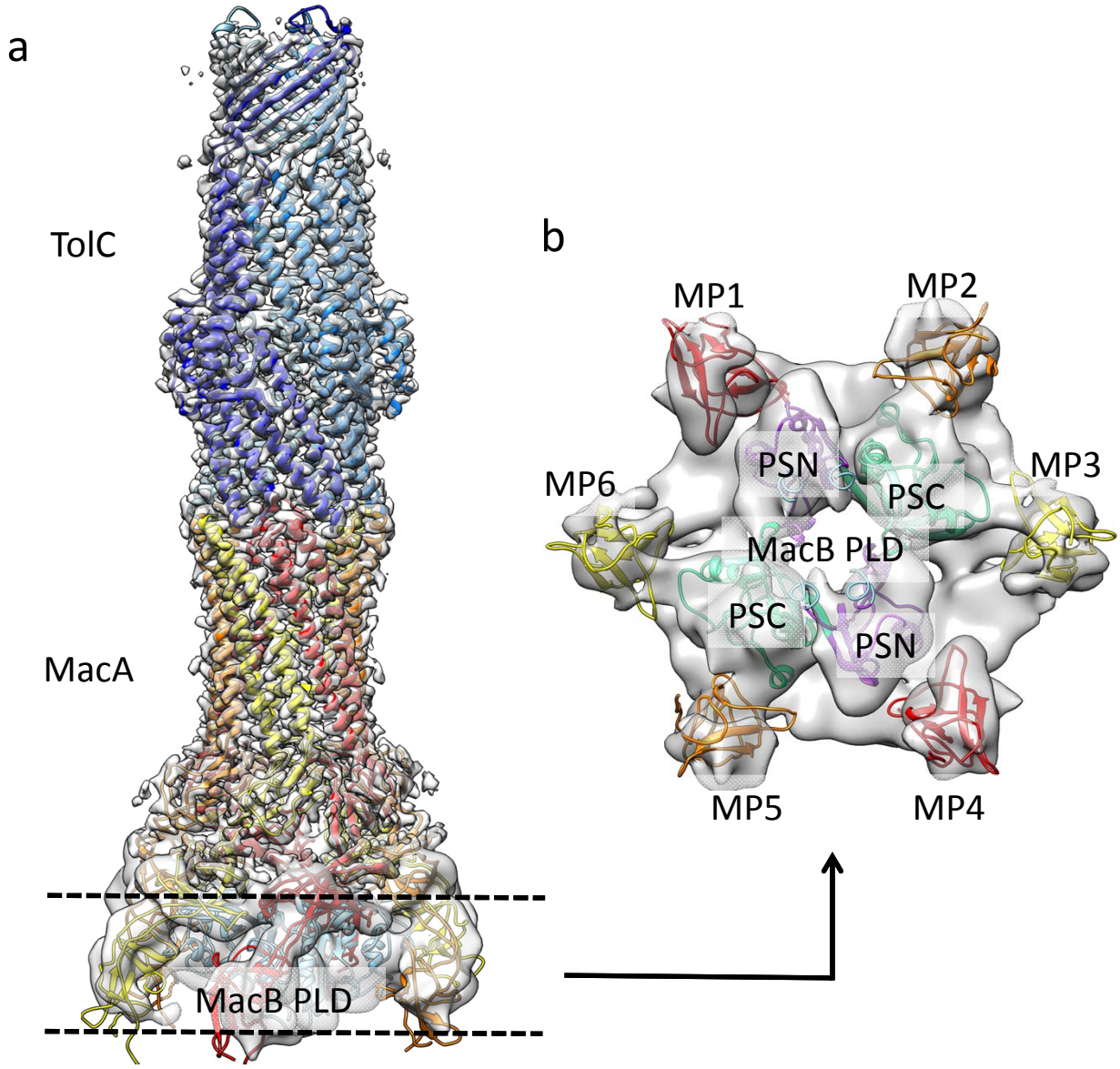


**Supplementary Figure 7 | Subunit stoichiometry of the MacAB-TolC pump.** **a,** CryoEM map of the disulfide-bond stabilised MacAB-TolC pump with fitted model of TolC, MacA and the periplasmic domain of MacB, showing 3:6:2 stoichiometry for TolC:MacA:MacB. The map is a hybrid of the separate maps for the MacA-TolC and MacA_MP-MacB_PLD portions shown in Supplementary Fig. 5b (See methods section). **b,** Segments of the cryoEM density map of the pump showing the fit of the periplasmic domain (PLD) of a MacB dimer and six membrane proximal (MP) domains of MacA. PSN: periplasmic subdomain N; PSC: periplasmic subdomain C.

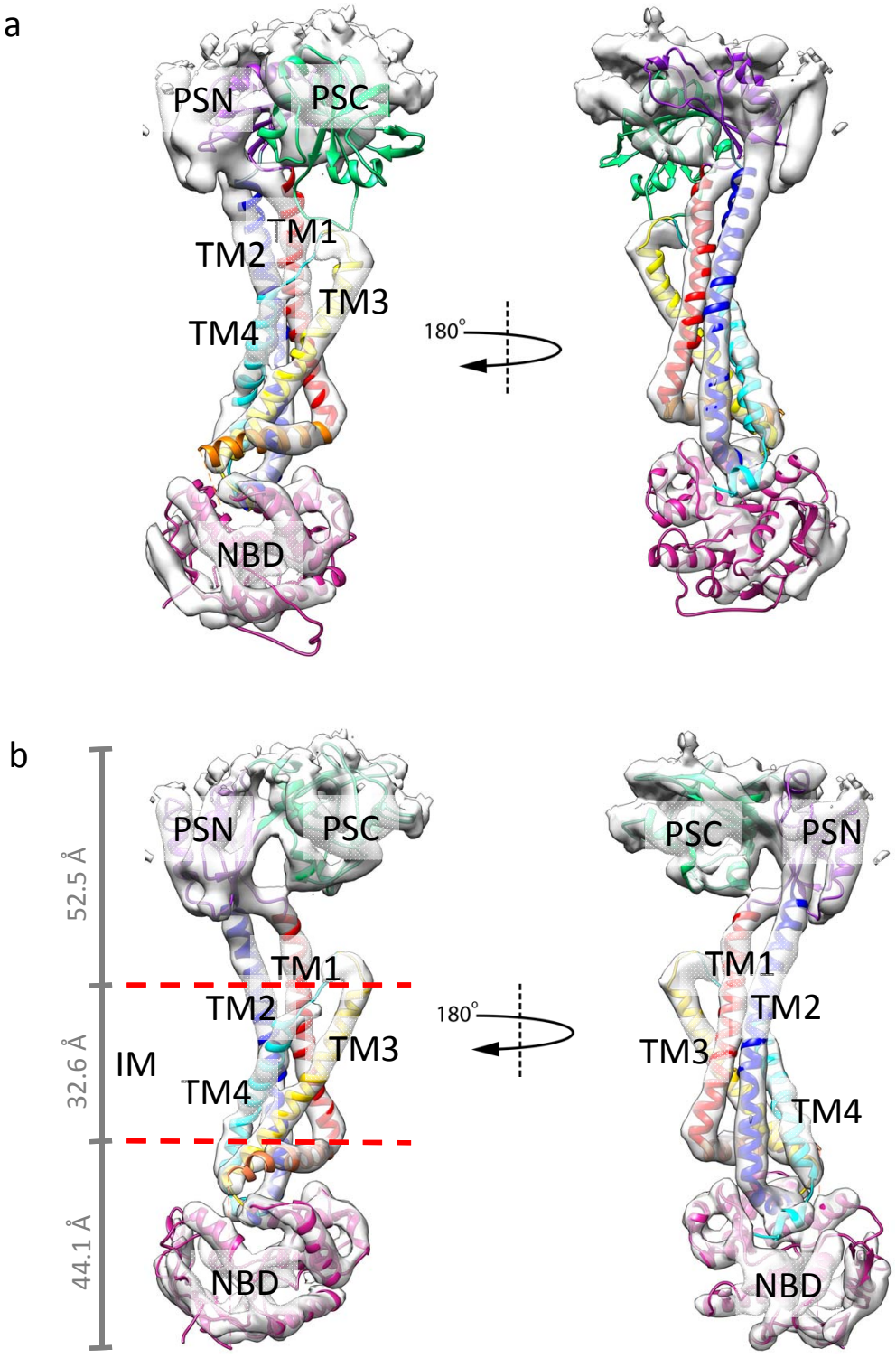


**Supplementary Figure 8 | Conformational difference between the crystal and cryo-EM structure of MacB. a,** Segments of the cryoEM density map for one MacB protomer with a fitted homology model built from the crystal structure shows mismatched PLD and NBD. **b,** Cryo-EM structure of MacB by rigid-body fitting of the PLD and NBD into the density map and refinement (See Methods section). There is a rotation of 180 degrees relating the views in the right and left panels. The dash lines delimit the boundary of inner membrane, with the NBD in the cytoplasmic side and the PLD (PSN and PSC) in the periplasmic side. PLD: periplasmic domain; PSN: periplasmic subdomain N; PSC: periplasmic subdomain C; NBD: nucleotide-binding domain; TM: transmembrane helix; IM: inner membrane.

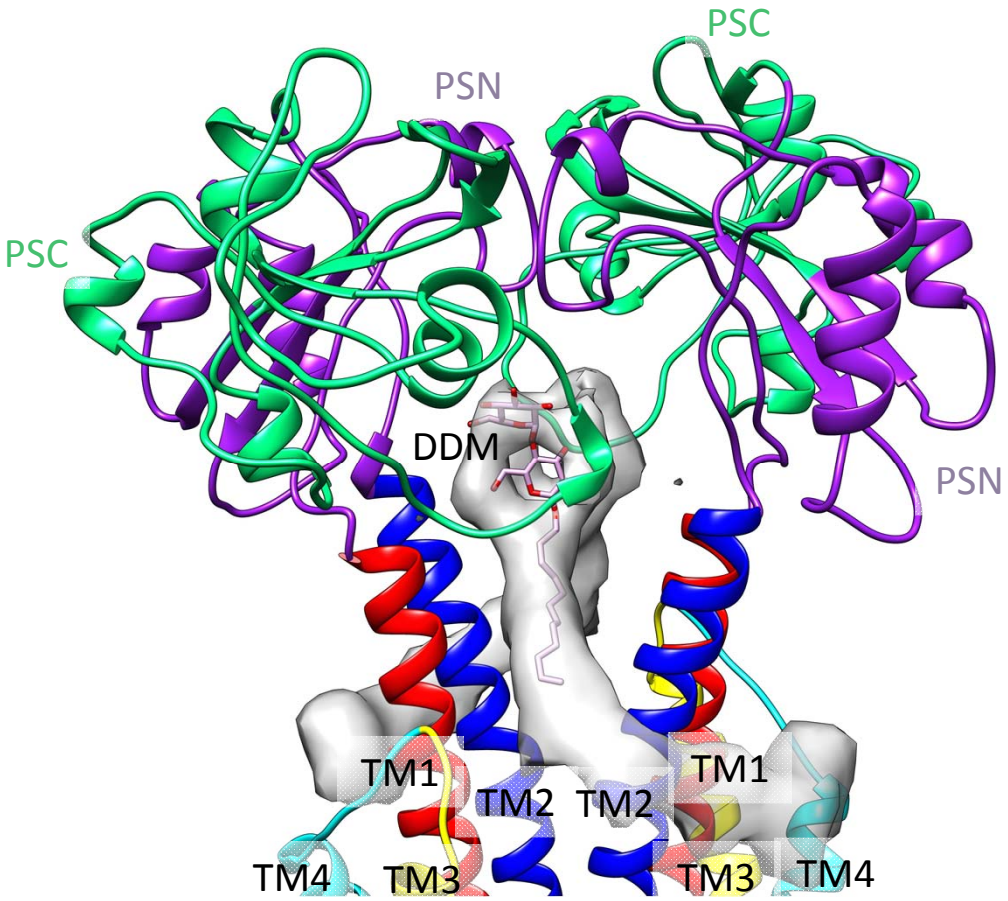


**Supplementary Figure 9 | Density occluding a potential periplasmic portal in the MacB.** Zoomed-in view of the unidentified, elongated density (grey) that occludes the portal region, showing mismatch of the dodecyl maltoside detergent molecule. PSN: periplasmic subdomain N; PSC: periplasmic subdomain C; TM: transmembrane helix; DDM: n-dodecyl-β-D-maltoside.

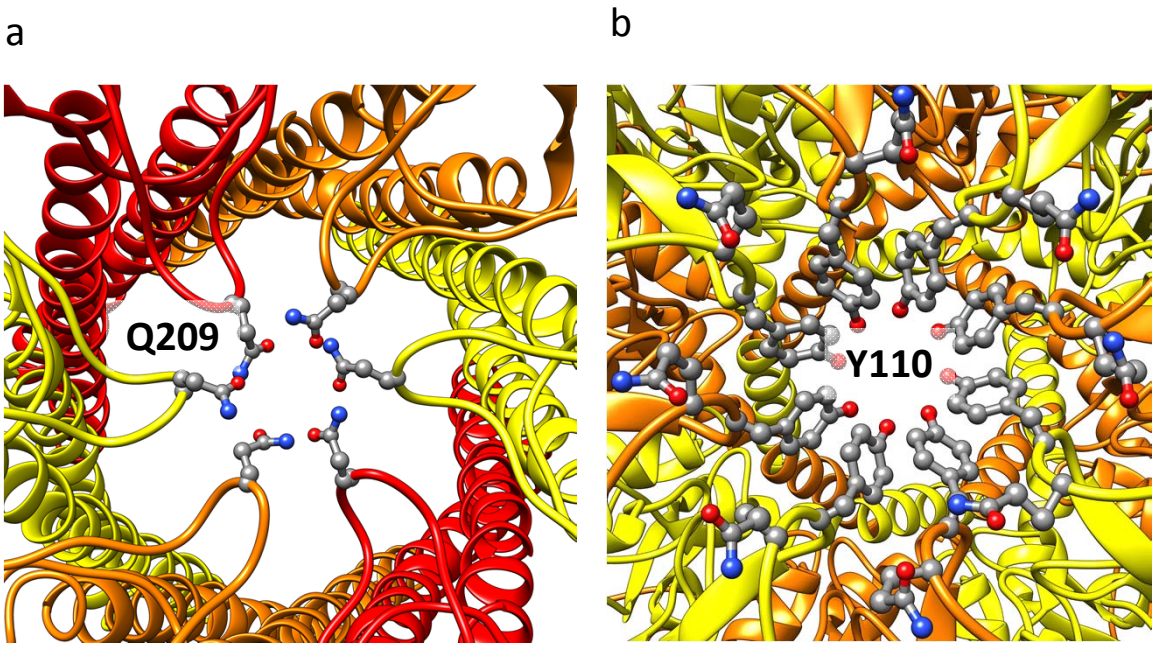


**Supplementary Figure 10** | **Gating rings of MacA and Wza.** **a,** Structure of *E.coli* MacA in the context of full pump assembly shows six glutamine residues (Q209) in the loops of lipoyl domains forming an inter-protomer hydrogen-bonding network. **b,** The hydrogen-bonding network between the tyrosines (Y110) of Wza protein (PDB access: 2J58).

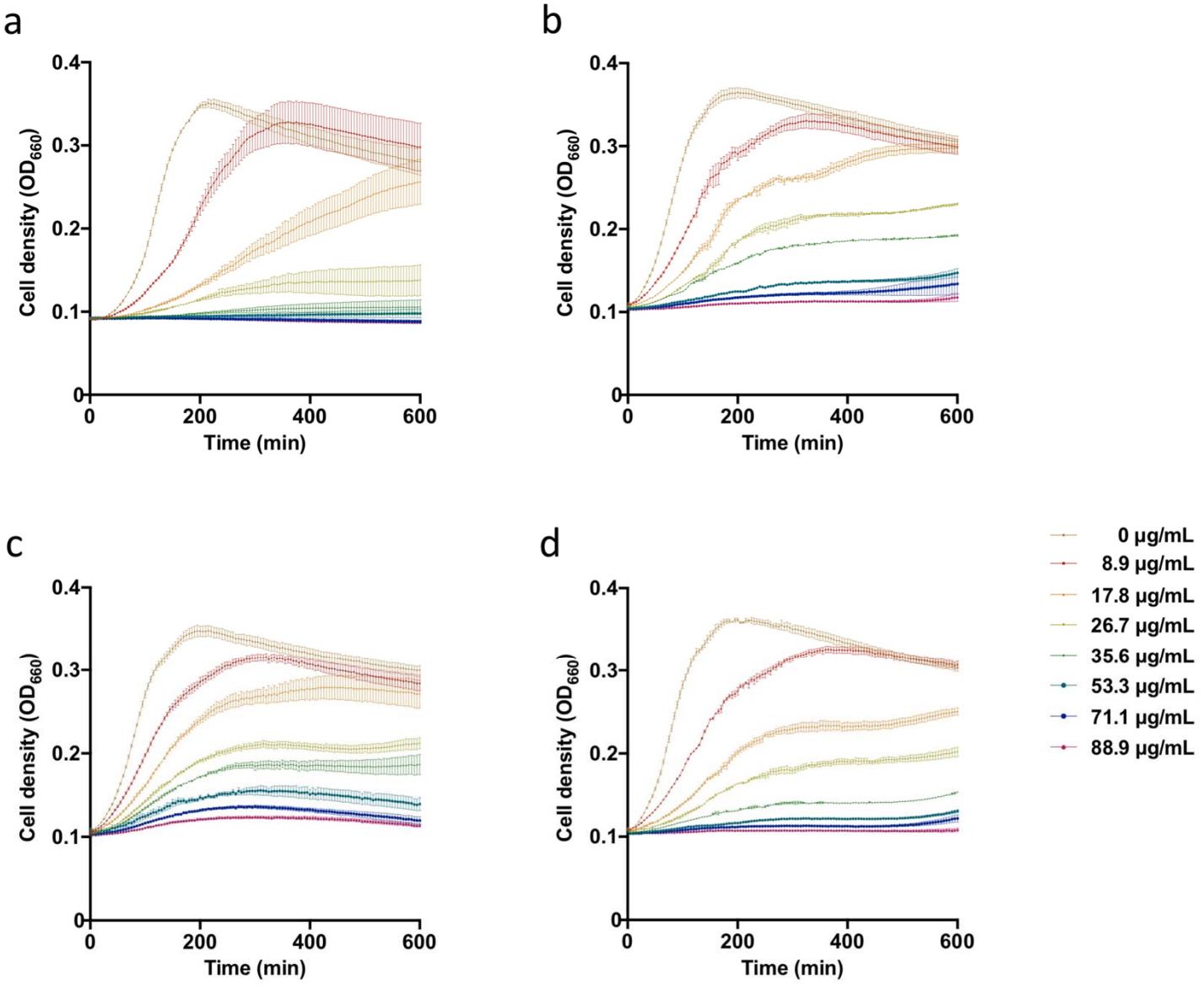


**Supplementary Figure 11 | Residues Q209 and Q210 are not required for efflux.** Growth of drug-hypersensitive *E. coli ΔacrAB* without MacAB expression (control) **a,** or with expression of wild-type MacAB **b,** MacA_Q209A MacB **c** or MacA_Q210A MacB **d** in the presence of 0 – 88.9 µg $ml^{-1}$ erythromycin. OD measurements are presented as mean of triplicate measurements ± standard error of the mean (SEM). The error bars/shaded regions represent standard error of the mean.

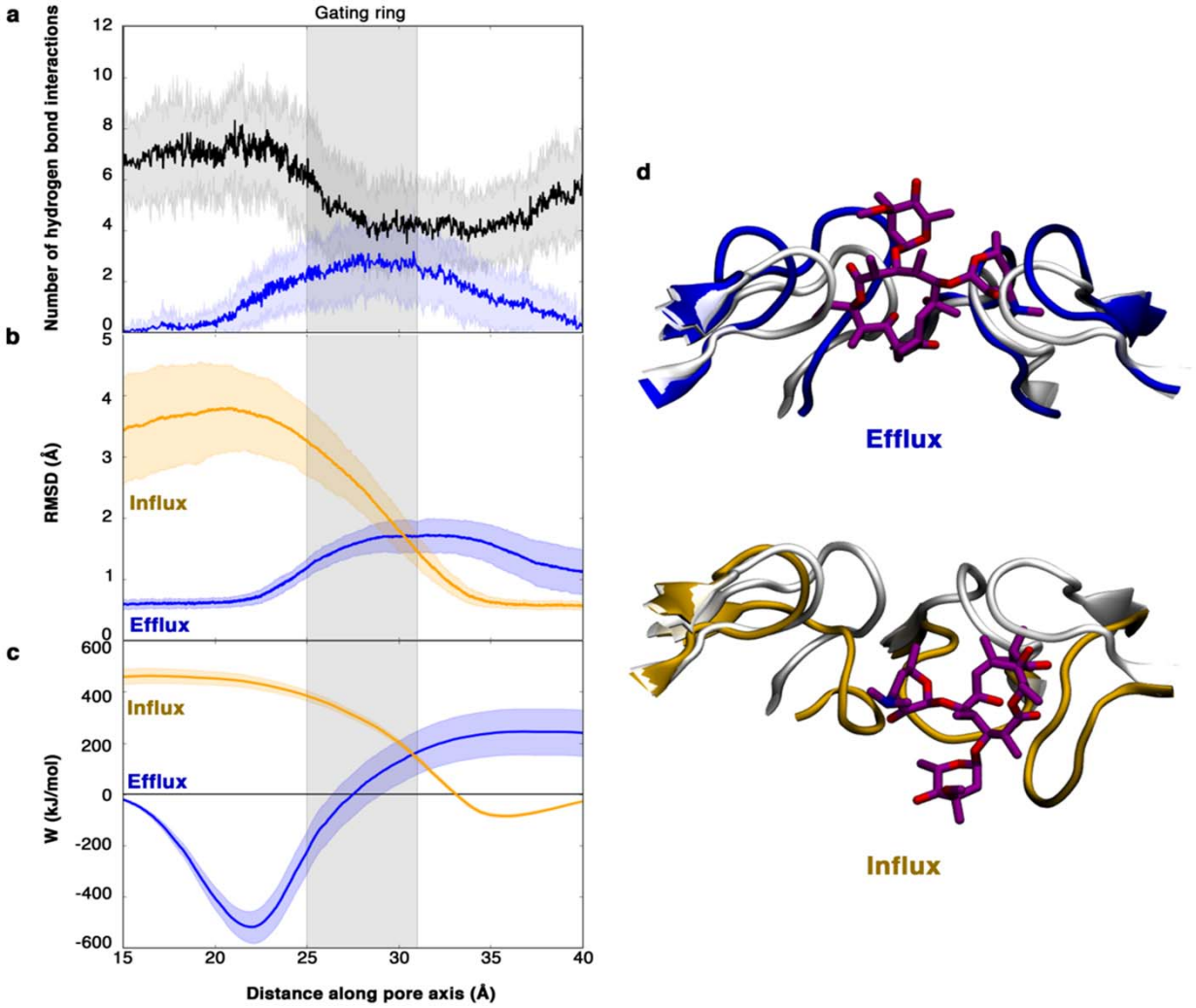


**Supplementary Figure 12 | Steered molecular dynamics simulations show passage of the substrate erythromycin through the MacA glutamine-gating ring during efflux and influx. a,** The hydrogen-bonding network between the loops, which forms a tight constriction in the pore (Fig. 1b), is partially replaced by hydrogen bonds with the substrate during transfer. The average number of inter-subunit hydrogen bonds between the loops in the hexamer (black, residues 203–215) and between the loops and erythromycin (blue) are shown as thick lines with their ± SD from 100 individual simulations as a shaded region. **b,** RMSD (average ± SD shown as thick lines and shaded regions, respectively) of the gating ring during passage of the substrate (Cα positions). Influx (ochre) induces a much larger distortion of the loops compared to efflux (blue). **c,** Averaged work profiles (± 95 % conf. interval, from 100 simulations in each direction shown as thick lines and shaded regions, respectively) recorded in steered MD simulations. Opening the gate for transfer of erythromycin in inward direction (ochre) requires the input of about 85 % more non-equilibrium work compared to erythromycin efflux. **d,** Representative conformations of the gating ring during efflux (top, blue) and influx (bottom, ochre) of erythromycin (magenta); the original conformation of the loops is shown in gray.

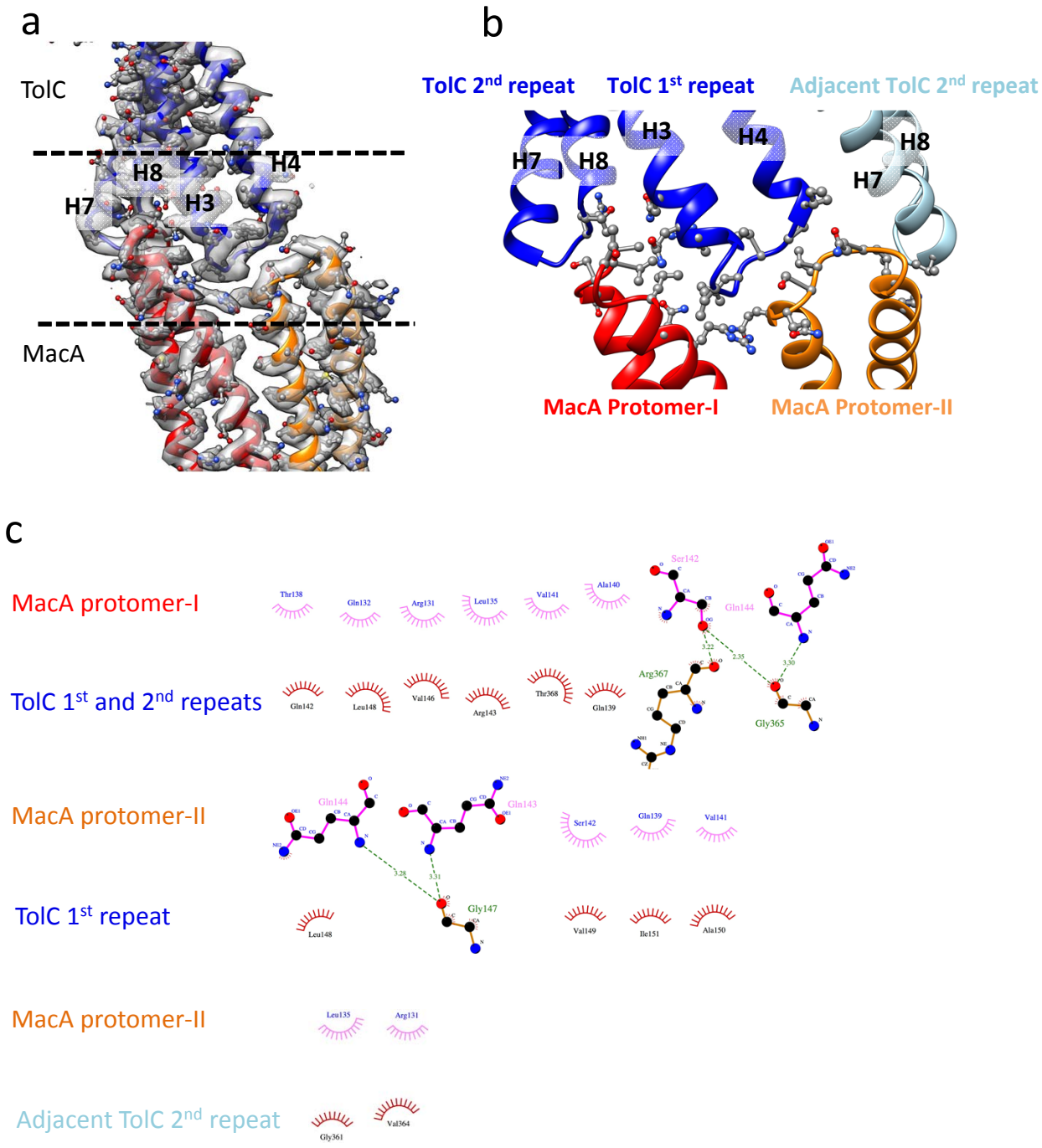


**Supplementary Figure 13 | Interactions between TolC and MacA in the MacAB-TolC pump. a,** Segments of the cryoEM density map of the pump with fitted model showing the tip-to-tip interaction between a TolC protomer (blue) and two α-helical hairpins of AcrA (Red and Orange). The side chains of residues are shown in ball & stick. **b,** Closer view of the region between the dash lines in **a**, showing the interaction interfaces between MacA and TolC. The side chains of residues involved in the interaction are shown in ball & stick. **c,** The detailed interactions are shown by LigPlot.

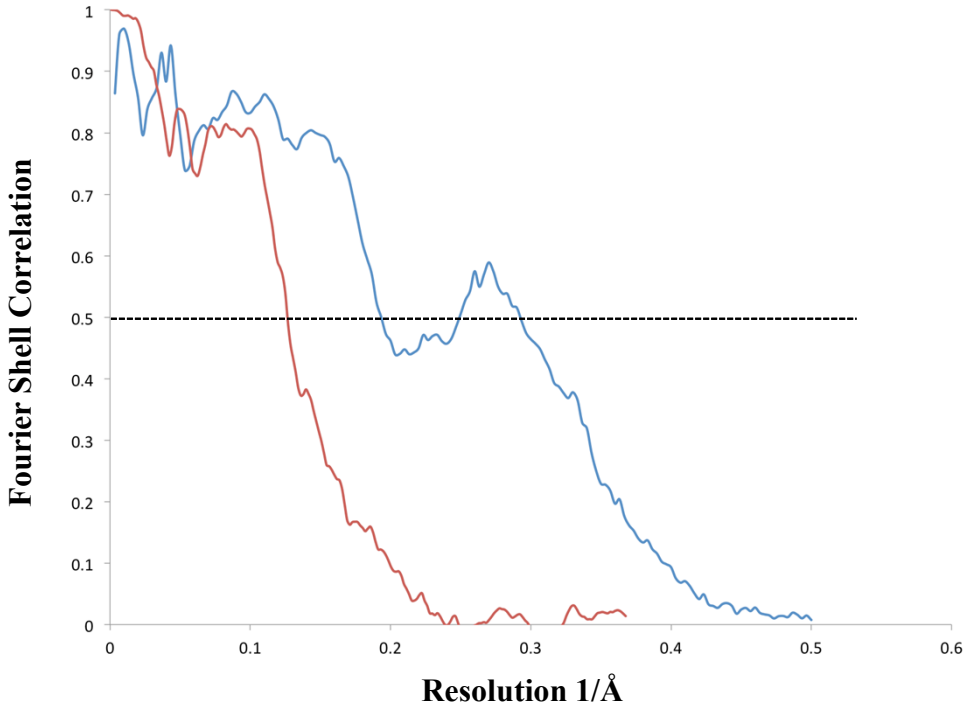


**Supplementary Figure 14 | The FSC curve between cryoEM density maps and the molecular models.** FSC curves of model versus map for the MacA-TolC (blue line) and MacB (red line). The curves show FSC between the model and the sum of the two half maps it was refined against.